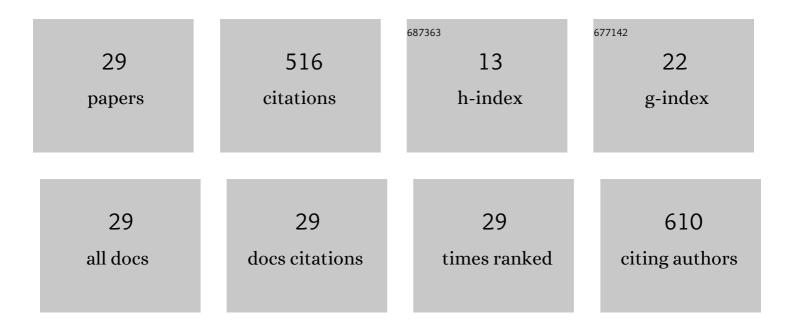
Anže Založnik

List of Publications by Year in descending order

Source: https://exaly.com/author-pdf/4065879/publications.pdf Version: 2024-02-01



AND34F 7110334NIK

#	Article	IF	CITATIONS
1	Plasma–wall interaction studies within the EUROfusion consortium: progress on plasma-facing components development and qualification. Nuclear Fusion, 2017, 57, 116041.	3.5	75
2	In situ NRA study of hydrogen isotope exchange in self-ion damaged tungsten exposed to neutral atoms. Journal of Nuclear Materials, 2016, 469, 133-144.	2.7	41
3	Hydrogen isotope accumulation in the helium implantation zone in tungsten. Nuclear Fusion, 2017, 57, 064002.	3.5	37
4	Retention and release of hydrogen isotopes in tungsten plasma-facing components: the role of grain boundaries and the native oxide layer from a joint experiment-simulation integrated approach. Nuclear Fusion, 2017, 57, 076019.	3.5	33
5	Simulations of atomic deuterium exposure in self-damaged tungsten. Nuclear Fusion, 2017, 57, 056002.	3.5	33
6	Displacement damage stabilization by hydrogen presence under simultaneous W ion damage and D ion exposure. Nuclear Fusion, 2019, 59, 086050.	3.5	32
7	The influence of the annealing temperature on deuterium retention in self-damaged tungsten. Physica Scripta, 2016, T167, 014031.	2.5	30
8	Deuterium atom loading of self-damaged tungsten at different sample temperatures. Journal of Nuclear Materials, 2017, 496, 1-8.	2.7	29
9	Deuterium retention in tungsten simultaneously damaged by high energy W ions and loaded by D atoms. Nuclear Materials and Energy, 2017, 12, 169-174.	1.3	28
10	Exercise-induced effects on a gym atmosphere. Indoor Air, 2016, 26, 468-477.	4.3	27
11	LIBS detection of erosion/deposition and deuterium retention resulting from exposure to Pilot-PSI plasmas. Journal of Nuclear Materials, 2017, 489, 129-136.	2.7	19
12	Influence of grain size on deuterium transport and retention in self-damaged tungsten. Journal of Nuclear Materials, 2019, 513, 198-208.	2.7	19
13	Stabilization of defects by the presence of hydrogen in tungsten: simultaneous W-ion damaging and D-atom exposure. Nuclear Fusion, 2019, 59, 016011.	3.5	14
14	In situ hydrogen isotope detection by ion beam methods ERDA and NRA. Nuclear Instruments & Methods in Physics Research B, 2016, 371, 167-173.	1.4	13
15	Growth mechanism of epitaxial SrTiO ₃ on a (1 × 2) + (2 × 1) reconstructed Sr(1/2 ML)/Si(001) surface. Journal of Materials Chemistry C, 2020, 8, 518-527.	5.5	13
16	Modeling the sharp deuterium release from beryllium co-deposits. Nuclear Fusion, 2019, 59, 126027.	3.5	11
17	The influence of helium on deuterium retention in beryllium co-deposits. Journal of Nuclear Materials, 2018, 512, 25-30.	2.7	10
18	Time-resolved laser-induced desorption spectroscopy (LIDS) for quantified <i>in-situ</i> hydrogen isotope retention measurement and removal from plasma facing materials. Review of Scientific Instruments, 2019, 90, 073502.	1.3	8

Anže Založnik

#	Article	IF	CITATIONS
19	Plasma-Material-Interaction Research Using PISCES Linear Plasma Devices. Fusion Science and Technology, 2019, 75, 664-673.	1.1	8
20	Experimental measurements and modeling of the deuterium release from tungsten co-deposited layers. Nuclear Materials and Energy, 2020, 23, 100743.	1.3	7
21	Micro-NRA and micro-3HIXE with 3 He microbeam on samples exposed in ASDEX Upgrade and Pilot-PSI machines. Nuclear Instruments & Methods in Physics Research B, 2017, 404, 179-184.	1.4	5
22	Deuterium retention in MeV ion-irradiated beryllium. Journal of Nuclear Materials, 2021, 555, 153139.	2.7	5
23	The influence of nitrogen co-deposition in mixed layers on deuterium retention and thermal desorption. Journal of Nuclear Materials, 2015, 467, 472-479.	2.7	4
24	Interaction of ammonia and hydrogen with tungsten at elevated temperature studied by gas flow through a capillary. Journal of Vacuum Science and Technology A: Vacuum, Surfaces and Films, 2017, 35, 061602.	2.1	4
25	Improved scaling law for the prediction of deuterium retention in beryllium co-deposits. Nuclear Fusion, 2022, 62, 036006.	3.5	4
26	Deuterium removal from beryllium co-deposits by simulated strike-point sweeping. Nuclear Materials and Energy, 2020, 24, 100750.	1.3	3
27	D retention and material defects probed using Raman microscopy in JET limiter samples and beryllium-based synthesized samples. Physica Scripta, 2021, 96, 124031.	2.5	2
28	Study of lateral distribution of impurities on samples exposed in the ASDEX Upgrade using microbeam of 3He and 1H. Physica Scripta, 2017, T170, 014067.	2.5	1
29	The influence of D <mml:math <br="" display="inline" xmlns:mml="http://www.w3.org/1998/Math/MathML">id="d1e302" altimg="si10.svg"><mml:msub><mml:mrow /><mml:mrow><mml:mn>2</mml:mn></mml:mrow></mml:mrow </mml:msub></mml:math> pressure on D retention and release from Be co-deposits. Nuclear Materials and Energy, 2021, 28, 101023.	1.3	1